Journal of Molecular Structure 963 (2010) 228–233

Contents lists available at ScienceDirect

Journal of Molecular Structure

journal homepage: www.elsevier.com/locate/molstruc

Self assembled pseudo double helix architecture and anion sensing behavior of a coumarin based ICT probe

K.K. Upadhyay [a,*], Rakesh K. Mishra [a], Ajit Kumar [a], Jianzhang Zhao [b], Rajendra Prasad [a]

[a] Department of Chemistry, Faculty of Science, Banaras Hindu University, Varanasi 221005, India
[b] State Key Laboratory of Fine Chemicals, Dalian University of Technology, Dalian 116012, China

ARTICLE INFO

Article history:
Received 19 September 2009
Received in revised form 22 October 2009
Accepted 22 October 2009
Available online 29 October 2009

Keywords:
ICT
Coumarin
Colorimetric
Anion recognition
DFT

ABSTRACT

The X-ray diffraction (XRD) studies of a coumarin based hydrazone (receptor 1) have revealed self assembled pseudo double helix architecture involving closed shell O—O interactions besides other supramolecular interactions. The receptor (1) an intramolecular charge transfer (ICT) probe detected acetate, benzoate and dihydrogenphosphate through naked-eye in DMSO. The 1:1 stoichiometry was confirmed for all the anions. The ^{1}H NMR studies indicated classical and non-classical hydrogen bonding through –NH and Ar–H protons of the receptor, respectively, during recognition process of the acetate through receptor (1). The theoretical studies through density functional theory (DFT) using B3LYP exchange functional with the basis set 6-311G** supported the UV–vis and ^{1}H NMR studies. The time dependent density functional theory (TDDFT) computations of UV–vis excitations for the receptor (1) and receptor–acetate complex agreed well with our experimental findings. The cyclic voltammetric studies also supported formation of receptor–acetate complex.

1. Introduction

Designing and synthesis of molecules exhibiting self assembled structures and having potential ability of structural/functional mimicry for bio-macromolecules are of current interest in the field of supramolecular chemistry [1]. The self assembled structures are interknitted through long range weak interactions such as hydrogen bonding, pi–pi and van der Walls interactions. These synthetic structural models are sometimes able to provide an insight towards the understanding of the structural and functional details of bio-macromolecules up to varying extent. Besides their job as role models towards the understanding of biochemical processes they have also been used for their possible applications in the field of analyte sensing, data storage [2], etc. Owing to a variety of applications in biochemical processes, pharmaceuticals, catalysis, environmental chemistry the carboxylate and dihydrogenphosphate anions constitute one of the important class of analyte [3]. Hence there has been a continuous growing interest of chemists towards the designing and synthesis of the chemoreceptor for anions [4]. Among the chemoreceptor the naked-eye ones have an edge over others in view of their cost effectiveness and simple experimental protocols.

Present study is a part of our current research interest towards synthesis and evaluation of some chemoreceptors for biologically relevant cations and anions involving simple reaction protocol [5]. The receptor being reported in this communication contains polarized –NH fragment on the skeleton of a coumarin containing hydrazone which behaves as H-bond donor towards anions [6]. Coumarin being part of the natural system has been exploited by supramolecular chemists in making it as one of the constituent of chemoreceptors for anions [7].

Although the receptor (1) has been synthesized and screened as a plant growth regulator earlier [8] but was never fully characterized. This is for the first time that we have revealed a unique self assembled double helix pattern in the receptor (1) through its X-ray diffraction (XRD) studies and pursued its anion sensing behavior through UV–vis and ^{1}H NMR spectral studies besides theoretical studies using density functional theory.

2. Experimental

2.1. Apparatus

^{1}H NMR spectra were recorded on a Bruker-400 Avance NMR Spectrometer. ESI-MS was carried out on a MDS Sciex API 2000 LCMS spectrometer. C, H and N elemental analysis were done on Model CE-440 CHN analyser. UV–vis spectra were recorded on a UV-1700 Pharmaspec spectrophotometer with quartz cuvette (path length = 1 cm) at 298 K.

2.2. Materials

All reagents for synthesis were purchased from Sigma–Aldrich and were used without further purification. The DMSO of HPLC

* Corresponding author. Tel.: +91 542 6702488.
E-mail address: drkaushalbhu@yahoo.co.in (K.K. Upadhyay).

0022-2860/$ - see front matter © 2009 Elsevier B.V. All rights reserved.
doi:10.1016/j.molstruc.2009.10.040

grade was purchased from Spectrochem Pvt. Ltd. Mumbai, India and was used for the preparation of solutions in the UV–vis titrations. The anions for UV–vis and ^{1}H NMR titrations purposes were taken as their tetrabutylammonium salts and purchased from Sigma–Aldrich Pvt. Ltd.

2.3. General Method

All UV–vis titration experiments were carried out at room temperature. To the 5×10^{-5} M DMSO solution of the receptor, the varying equivalents of the anions were added separately and spectra were recorded. Titration plots were generated by using Origin 5.0 (Microcal software). The binding constants were calculated by using custom-written non-linear least-squares curvefitting program implemented within Sigma Plot 2000 (SPSS Inc.). The ^{1}H NMR titrations were carried out in DMSO-d_6 using TMS as an internal reference standard. To the 5×10^{-3} M solution of the receptor in DMSO-d_6 the varying equivalents of acetate as its tetra butyl ammonium salt were added and the ^{1}H NMR spectra recorded after each addition.

2.4. Synthesis of receptor (1)

Receptor (1) was synthesized by adding an ethanolic solution of 2,4-dinitrophenylhydrazine (DNP) (2.0 mmol) to the equimolar ethanolic solution of 3-acetylcoumarin having one drop of HCl followed by constant stirring. The stirring of the reaction mixture was further continued for ~2 h with mild heating at 60 °C (Scheme 1). An orange colored solid was precipitated which was filtered followed by its recrystallization with ethanol–water mixture (50% v/v) and finally dried under vacuum over anhydrous $CaCl_2$. Receptor (1) was characterized by single-crystal XRD besides ^{1}H NMR, ESI-MS, IR, and elemental analysis. 3-Acetyl coumarin was synthesized by reported method [9]. Ethyl acetoacetate (0.01 mol), taken in conical flask was chilled in an ice-bath and treated with a drop of piperidine. To this was added salicylaldehyde (0.01 mol) and the mixture was cooled and shaken for 2 h when the colorless solid appeared. The crude product was recrystallized from aqueous ethanol, dried and was used for further synthesis. Yield: 92%.^{1}H NMR (400 MHZ, DMSO-d_6, 298 K, TMS): δ 11.09 (1H, s, HN–), 8.91 (d, 1H, H-Ar), 8.45 (s, 2H, H–Ar), 8.07 (d, 1H, H–Ar), 7.89 (d, 1H, H–Ar), 7.69 (t, 1H, H–Ar), 7.40 (m, 2H, H–Ar), 2.43 (s, 3H, CH_3), ESI Mass: m/z Calculated for $C_{17}H_{12}N_4O_6$ [M]: 368.00, found: [M–H]- 367.1, [M+H]- 369.3, CHN(%): Calculated: C = 55.44, H = 3.28, N = 15.21, O = 26.06. Found: C = 55.77, H = 3.44, N = 15.06, O = 25.74.

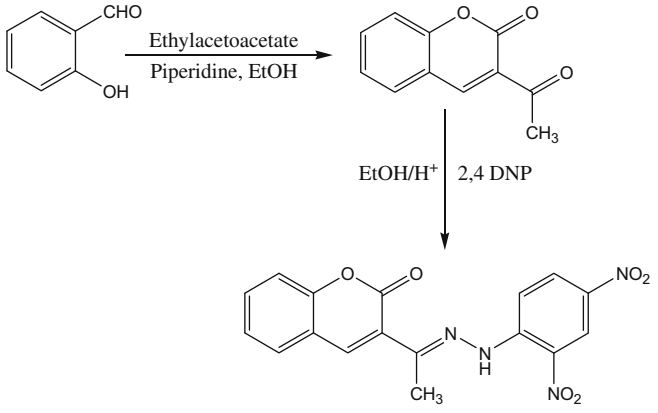

Scheme 1. Synthesis of receptor (1).

2.5. X-ray diffraction studies (1)

Suitable crystals of the receptor (1) were obtained from slow evaporation of a supersaturated solution of the receptor (1) in the chloroform covered with diethyl ether. Single-crystal X-ray data were collected at 100 K on a Bruker SMART APEX CCD diffractometer using graphite-monochromated MoKα radiation (k = 0.71073 Å). The linear absorption coefficients, scattering factors for the atoms, and the anomalous dispersion corrections were taken from International Tables for X-ray Crystallography. The data integration and reduction were processed with SAINT [10] software. An empirical absorption correction was applied to the collected reflections with SADABS [11] using XPREP [12]. The structure was solved by the direct method using SHELXTL [13] and was refined on F^2 by full matrix least-squares technique using the SHELXL-97 [14] program package. For all the cases non-hydrogen atoms were refined anisotropically. The hydrogen atoms were geometrically fixed and treated as riding atoms using SHELXL default parameters.

3. Results and discussion

3.1. X-ray diffraction studies

Each unit cell embodies four receptor molecules with two types of prominent long range interactions. The lactone ring of one receptor molecule undergoes pi stacking with dinitrophenyl ring of another receptor (head to tail recognition) with intercentreoid distance of 3.66 Å. Other long range interaction involves C_{11}–H of one receptor with C_6 of the other receptor with a distance of 2.68 Å. The inter unit cell long range interactions are more prominent. The C_{14} of one receptor interacts with C_5 of another receptor at a distance of 3.39 Å. The π–π interaction between benzene ring of one receptor takes place with dinitrophenyl ring of another receptor (head to tail recognition) having intercentreoid distance 3.72 Å.

The above interactions lead to formation of individual strands while the pseudo double helix formation takes place through long range O_2—O_4 closed shell interaction with a distance of 2.82 Å which is less than the twice of van der Waals radius of oxygen atom and matches with the literature report for this type of interaction [15]. A constant distance of ~21.5 Å is maintained between the repeating groves or ridges through out the entire structure (Supplementary Information, Fig. S13). Important crystallographic data have been given in Supplementary Information (Table S14) while the ORTEP representation of X-ray crystal structure of the receptor (1) along with its self assembled pseudo double helix structure have been shown in Fig. 1(A) and (B), respectively.

3.2. UV–visible studies

The 5×10^{-5} M DMSO solution of the receptor (1) itself absorbs in the form of broad band at 395 nm and visibly appeared yellow. The respective additions of 1 equivalent of the chosen anions as their tetrabutyl ammonium salts to this receptor solution was able to produce visible color change from yellow to purple only in the cases of carboxylate ones and dihydrogenphosphate (Fig. 2A). The remaining less basic anions like hydrogensulfate, perchlorate, hexaflurophosphate and tetrafluroborate were not able to do so.

The UV–vis scanning of the receptor solution having carboxylate/dihydrogenphosphate showed vanishing of the signal at 395 and origin of a new signal at 535 nm. Though the intensity of the purple color varied and followed the relative basicity order of acetate, benzoate and dihydrogenphosphate. Although benzoate is superior to dihydrogenphosphate in terms of basicity [16] but

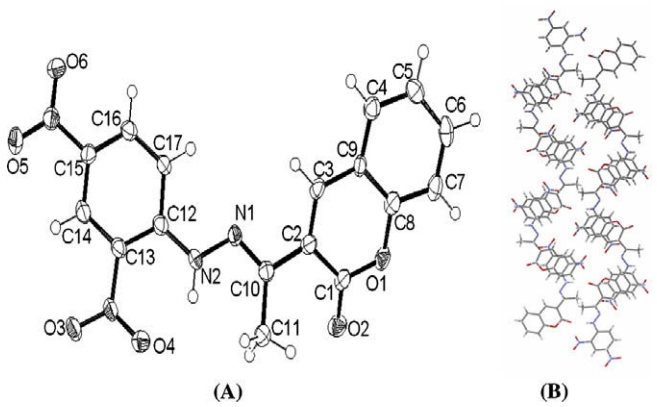

Fig. 1. (A) ORTEP representation of X-ray crystal structure of receptor (1) (displacement ellipsoids are scaled to the 50% probability level). (B) Pseudo double helical structure of the receptor (1) along a axis (wireframe model).

showed almost equal intensity possibly due to its favorable structure for the interaction on the similar line of a literature report. This large bathochromic shift of 140 nm may be a consequence of deprotonation of –NH proton of the receptor on the addition of anion. The comparative intensity of 535 nm UV–vis band of the 5×10^{-5} M DMSO solution of receptor (1) on the respective addition of 1 equivalent of different anions as their tetraburyl ammonium salts have been given in Fig. 2(B) and in terms of bar chart shown in Fig. 2(C).

A representative UV–vis spectrum of the receptor (1) on concomitant addition of acetate along with binding curve from corresponding titration data have been given in Fig. 3(A) and (B). Two clear isosbestic points at 442 and 320 nm were observed. The job's plot showing 1:1 stoichiometry for the binding of acetate with receptor (1) has been given in the inset of Fig. 3B. The corresponding UV–vis spectral information for the titrations of rest of the ions with receptor (1) has been appended in the form of Supplementary Material (Figs. S1–S7). The occurrence of isosbestic points at the same wavelength position for all the chosen anions indicated that the receptor–anion complex equilibria are similar for all of them.

The corresponding binding constants K_a (M^{-1}) for the receptor–anion complexes were determined by non-linear fitting analyses of the UV–vis titration data according to the equation for 1:1 complexation reported in literature [17] and have been given in Table 1.

$$A = Ao + (A_{lim} - Ao)/2Co[Co + Cm + 1/K_a - (Co + Cm + 1/K_a)^2 - (4CoCm)^{1/2}] \quad (1)$$

where, A: absorbance of the solution during the titration, Ao: absorbance of the ligand, A_{lim}: absorbance of the ML complex, Co: concentration of the ligand, Cm: concentration of the anion during the titration, K_a: equilibrium constant of the complex formation.

3.3. ^1H NMR studies

As the UV–vis spectral titrations discussed above indicated 1:1 complexation between the receptor 1 and all the chosen anions. Hence, a representative anion as acetate was chosen in order to understand the probable binding sites on the receptor 1 through ^1H NMR spectral titrations. The partial ^1H NMR spectra for the titration between 5×10^{-3} M in DMSO-d_6 solution of the receptor (1) and varying equivalents of acetate as tetra butyl ammonium salt have been given in Fig. 4A. On addition of 0.25 equivalent of tetra butyl ammonium acetate to the solution of the receptor (1), the –NH proton and the Ar–H_b showed broadening and downfield shifting accompanied by emergence of a new signal at 9.86 δ ppm. Thus an intermediate structure where the acetate forms a bridge between NH and Ar–H_b protons of the receptor

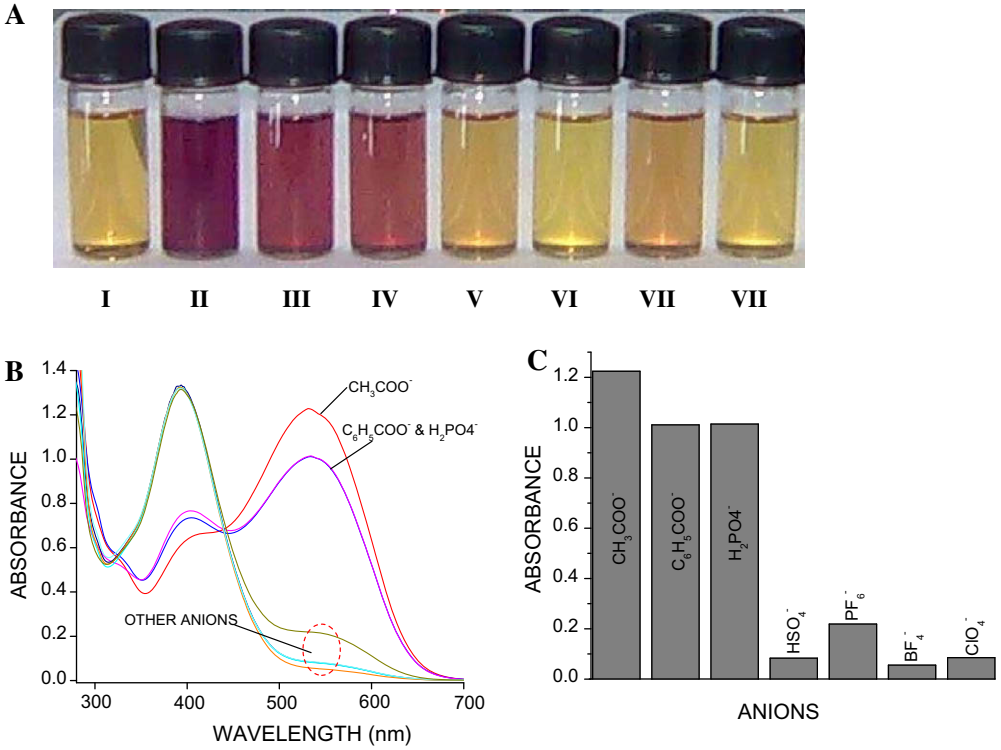

Fig. 2. (A) Color changes of receptor (1) (5×10^{-5} M) in DMSO on addition of 1 equivalent each of tetrabutylammonium salts of anions: (I) free receptor (1), (II) Acetate, (III) Benzoate, (IV) dihydrogen phosphate, (V) hydrogensulfate, (VI) perchlorate, (VII) hexaflurophosphate, (VIII) tetrafluroborate. (B) Corresponding UV–vis spectral changes of receptor (1) in DMSO solution (5×10^{-5} M) with the addition of 1.00 equivalent. (C) Bar graph representation of spectral changes at 535 nm.

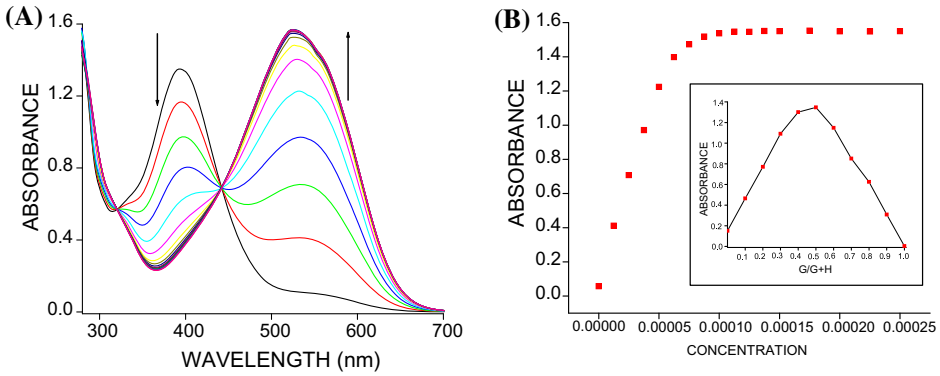

Fig. 3. (A) Changes in the electronic spectra for DMSO solutions of receptor (1) (5×10^{-5} M) on concomitant addition of tetrabutylammonium acetate. (B) Binding curve from corresponding titration data and job's plot (inset).

Table 1
The association constants K_a [M^{-1}] obtained from UV–vis titration for receptor (1) and anion complexes.

Anions[a]	CH_3COO^-	$C_6H_5COO^-$	$H_2PO_4^-$	HSO_4^-	ClO_4^-	PF_6^-	BF_4^-
K (M^{-1})	$(3.01 \pm 0.01) \times 10^5$	$(1.84 \pm 0.09) \times 10^5$	$(1.91 \pm 0.06) \times 10^5$	n.d.	n.d.	n.d.	n.d.

n.d., not determined due to small spectral changes.
[a] All the anions have been used as their tetrabutyl ammonium salts.

may be proposed at this stage (Fig. 4B). The other aromatic protons shifted to upfield. On further addition of acetate the –NH proton got vanished while the Ar–H_b proton joined the other Ar–H protons in their upfield shift. The interaction of –NH and Ar–H_b proton with acetate lead an increase in electron density on arene protons both ways leading to their upfield shift which is constantly maintained throughout the further addition of acetate to the receptor. This vanishing of –NH proton and reversal of Ar–H_b to upfield δ ppm maybe understood in terms of complete loss of –NH proton and subsequent enhancement of electron density over arene protons, respectively. Hence the ^{1}H NMR studies indicated the participation of the Ar–H_b besides the –NH towards the binding of acetate by the receptor.

3.4. Density functional theory (DFT) studies

To understand the geometry of the receptor–acetate complex, the density functional theory (DFT) calculations with B3LYP exchange functional using 6-311G** basis set through Gaussian 03 package [18] have been carried out. The DFT optimized geometrical configurations of the receptor (1) and the receptor–acetate complex have been given in Figs. 5(A) and 6(A), respectively. As it can be seen from Fig. 6(A) that –NH proton of the receptor molecule is deprotonated with an acetate forming acetic acid which is involved in hydrogen bonding interaction with deprotonated receptor R–N^-———HOAc (1.906 Å) confirming our conclusion from ^{1}H NMR titrations.

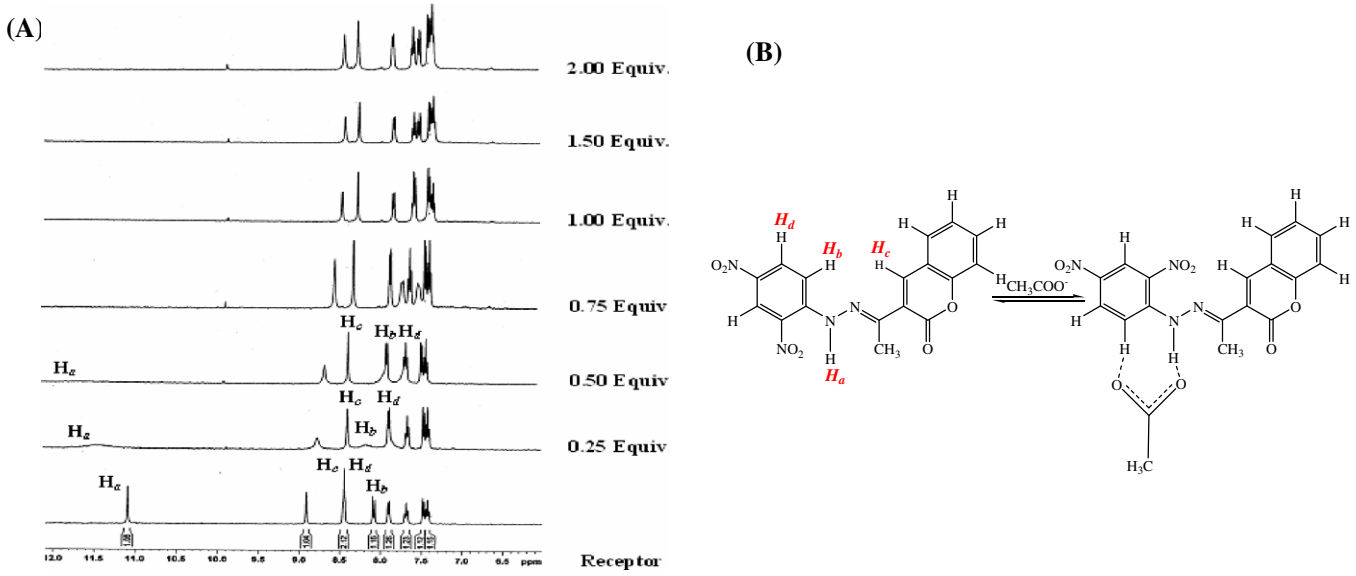

Fig. 4. (A) Partial ^{1}H NMR spectra showing changes in receptor (1) on concomitant addition acetate.(B) Chemical structure images for possible binding mode of receptor (1) with acetate anion.

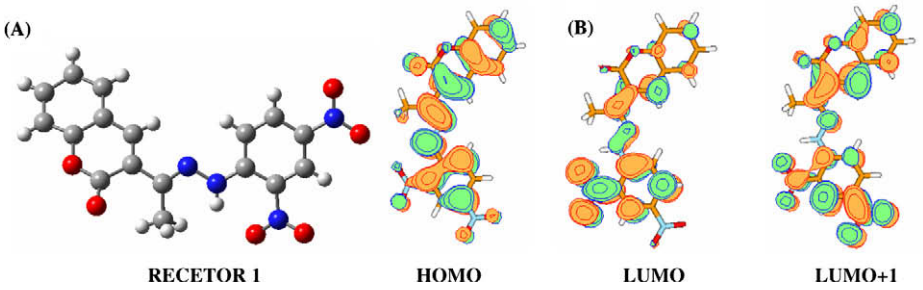

Fig. 5. (A) Optimized geometrical configuration receptor (1). (B) Kohn–Sham orbitals showing relevant MOs of the receptor (1) involved in UV–vis transitions.

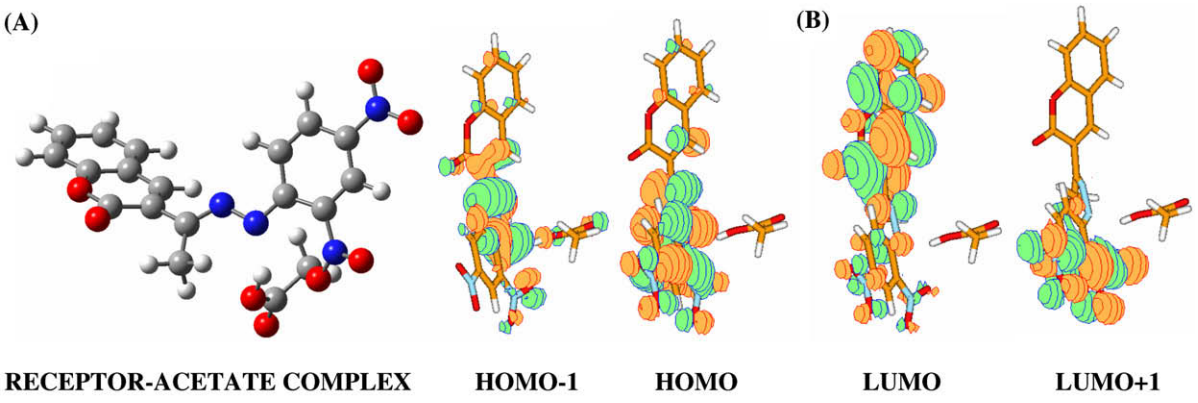

Fig. 6. (A) Optimized geometrical configuration receptor–acetate complex. (B) Kohn–Sham orbitals showing relevant MOs of the receptor–acetate complex involved in UV–vis transitions.

The natural bond orbital (NBO) analysis (Supplementary Information, Fig. S8) performed at the optimized geometry of the receptor (1) indicated that the DNP ring is electron rich (Donor, D) while the coumarin ring is electron deficient one (Acceptor, A) fulfilling the basic requirement of a push–pull i.e. D–π–A system [19]. The time dependent density functional theory (TDDFT) calculations for the excited state of receptor along with the receptor–acetate complex have also been performed. The Kohn–Sham orbitals involved in electronic transitions and responsible for the UV–vis absorption band of the receptor (1) have been shown in the Fig. 5(B). The HOMO and LUMO + 1 are delocalized over entire molecule while the LUMO is mainly concentrated over the donor part of the receptor. The receptor itself absorbed in the form of a broad band centered at 395 nm with its full width at half maximum (fwhm) ~100 nm leading to the range of the same band 345–445 nm. On the other hand the computed electronic transitions of two lowest energies for the receptor were found at 382 nm (HOMO → LUMO) and 422 nm (HOMO → LUMO + 1) with high intensities due to charge transfer from donor to acceptor. Hence the UV–vis absorption band at 395 nm may be taken as the composite band of these two transitions.

The HOMO and LUMO + 1 of the receptor–acetate complex are localized mainly over donor part of the receptor (1) while LUMO is concentrated over the acceptor part (Fig. 6B). The receptor–acetate complex absorbs at 535 nm in the form of a broad band with its full width at half maximum (fwhm) ~150 nm leading to the range of this band 450–610 nm. The computed bands were found at 478 (HOMO → LUMO) and 580 (HOMO − 1 → LUMO) nm fell well with in the experimental range of 450–610 nm. Nevertheless the computed band at 445 nm matched quite well with a shoulder at 441 nm in the UV–vis spectrum of receptor–acetate complex and this may be assigned due to HOMO → LUMO + 1 transition.

The relative energy level diagram of the relevant MOs of receptor and receptor–acetate complex (Supplementary Information, Fig. S9) clearly showed that all the MOs are raised in terms of their potential energy on complex formation with the acetate. The energy gap between the orbitals involved in UV–vis transitions have been decreased on formation of 1:1 complex with acetate. This very decrease in the energy gap of the relevant MOs is responsible for the bathochromic shift of the UV–vis band of the receptor from 395 to 535 nm on its interaction with acetate.

3.5. Cyclic voltammetric studies

In order to explore the possibility of the receptor (1) to be used as an electrochemical sensor the cyclic voltammetric studies were also

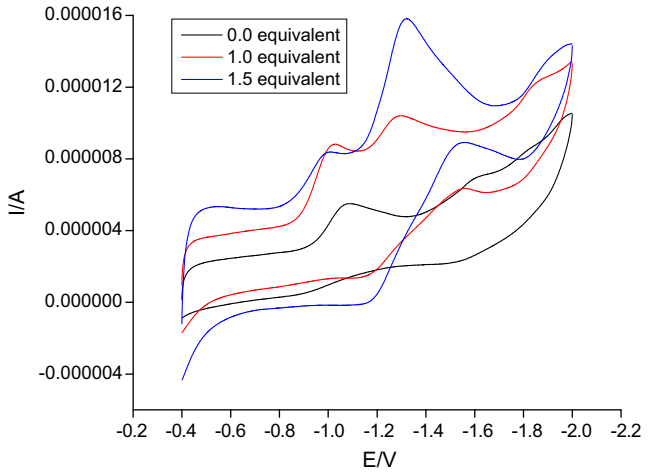

Fig. 7. Cyclic voltammogram of receptor (1) (DMSO 5×10^{-5} M) on concomitant addition of CH_3COO^- (working electrode: glassy carbon, reference electrode: Ag/Ag^+, counter electrode: Pt wire, supporting electrolyte: n-Bu_4NClO_4. Scan rate 100 mV s^{-1}).

performed. The cyclic voltammogram (Fig. 7) of the receptor produced anodic and cathodic peaks at −1.60 and −1.51 V, respectively, with a pre-adsorption wave at −1.06 V in the anodic region possibly due to adsorption of the receptor on the electrode surface. On the addition of 1.5 equivalent of acetate as its sodium salt, anodic and the cathodic wave shifted to −1.31 and −1.16 V, respectively. Besides the shifting of anodic and cathodic waves, the pre-adsorption wave was also shifted to −0.98 V as compared to −1.06 V in the free receptor. The shifting of anodic and cathodic waves towards less −ve potential on the addition of acetate to the receptor solution indicated a binding between receptor and acetate confirming our observation from UV–vis, ^{1}H NMR and DFT studies. At the same time it may also be concluded that after the binding of receptor with acetate it becomes more prone towards its adsorption at the electrode surface in the light of shifting of pre-adsorption wave towards less −ve potential. Hence the receptor (1) possesses potential ability to be used as an electrochemical sensor also.

4. Conclusion

Thus, we present a coumarin based hydrazone (receptor 1) having an exotic self assembled pseudo double helical supramolecular architecture in its solid state with its ability to act as ICT probe for the naked-eye detection of a few biologically relevant anions in dimethyl sulphoxide.

Acknowledgments

KKU gratefully acknowledges the financial help from UGC [F. No. 33-274/2007(SR)] and CSIR [No.01(2258)/08/EMR-II], New Delhi while R.K.M. and A.K. acknowledge gratefully the financial support from CSIR, New Delhi. Authors are thankful to the coordinator S.A.P.,DepartmentofChemistry,BHUforenablingGaussian03package.

Appendix A. Supplementary data

Supplementary data associated with this article can be found, in the online version, at doi:10.1016/j.molstruc.2009.10.040.

References

[1] V.R. Naidu, M.C. Kim, J. Suk, H. Kim, M. Lee, E. Sim, K. Jeong, Org. Lett. 10 (2008) 5373.
[2] F.J. Himpsel, A. Kirakosian, J.N. Crain, J.-L. Lin, D.Y. Petrovykh, Solid State Commun. 117 (2001) 149.
[3] (a) L. You, R. Ferdani, R. Li, J.P. Kramer, R.E.K. Winter, G.W. Gokel, Chem. Eur. J. 14 (2007) 382;
(b) S. Carvalho, R. Delgado, M.G.B. Drew, V. Calisto, V. Felix, Tetrahedron 64 (2008) 5392;
(c) M. Komiyama, M.L. Bender, M. Utaka, A. Taked, Proc. Natl. Acad. Sci. 74 (1977) 2634;
(d) A.F.D. de Namor, M. Shehab, J. Phys. Chem. A 108 (2004) 7324.
[4] (a) R. Martınez-Manez, F. Sancenon, Chem. Rev. 103 (2003) 4419;
(b) P.D. Beer, P.A. Gale, Angew. Chem. 40 (2001) 486;
[c] Special issue, Coord. Chem. Rev., 2003, 2006.;
(d) R.M.F. Batista, E. Oliveira, C. Nunez, S.P.G. Costa, C. Lodeiro, M.M.M. Raposo, J. Phys. Org. Chem. 22 (2009) 362.
[5] (a) K.K. Upadhyay, A. Kumar, S. Upadhyay, R.K. Mishra, P.K. Roychoudhuary, Chem. Lett. 37 (2008) 186;
(b) K.K. Upadhyay, A. Kumar, R.K. Mishra, R. Prasad, Bull. Chem. Soc. Jpn. 82 (2009) 813;
(c) K.K. Upadhyay, S. Upadhyay, K. Kumar, R. Prasad, J. Mol. Struct. 927 (2009) 60;
(d) F. Han, L. Chi, X. Liang, S. Ji, S. Liu, F. Zhou, Y. Wu, K. Han, J. Zhao, T.D. James, J. Org. Chem. 74 (2009) 1333.
[6] V. Amendola, D. Estenban-Gomez, L. Fabbrizzi, M. Licchelli, Acc. Chem. Res. 39 (2006) 343.
[7] (a) H. Miyaji, H.-K. Kim, E.-K. Sim, C.-K. Lee, W.-S. Cho, J.L. Sessler, C.-H. Lee, J. Am. Chem. Soc. 127 (2005) 12510;
(b) K.-S. Lee, H.-J. Kim, G.-H. Kim, I. Shin, J.-I. Hong, Org. Lett. 10 (2008) 49.
[8] V. Alexieva, I. Sergiev, I. Manolove, E. Karanow, Physiol. Plant. 55 (2002) 91.
[9] F. Knoevenagel, Ber. Dtsch. Chem. Ges. 31 (1898) 732.
[10] SAINT+, 6.02 ed., Bruker AXS, Madison, WI, 1999.
[11] G.M. Sheldrick, SADABS: Empirical Absorption Correction Program, University of Göttingen, Göttingen, Germany, 1997.
[12] XPREP, 5.1 ed., Siemens Industrial Automation Inc., Madison, WI, 1995.
[13] G.M. Sheldrick, SHELXTLTM Reference Manual, version 5.1., Bruker AXS, Madison, WI, 1997.
[14] G.M. Sheldrick, SHELXL-97: Program for Crystal Structure Refinement, University of Göttingen, Göttingen, Germany, 1997.
[15] Ian Dance, New J. Chem. 27 (2003) 22.
[16] (a) S. Nishizawa, P. Buhlmann, M. lwao, Y. Umezawa, Tetrahedron Lett. 36 (1995) 6483;
(b) N. Pelizzi, A. Casnati, A. Friggeri, R. Ungaro, J. Chem. Soc. Perkin Trans. 2 (1998) 1307.
[17] J. Bourson, J. Pouget, B. Valeur, J. Phys. Chem. 97 (1993) 4552.
[18] M.J. Frisch, G.W. Trucks, H.B. Schlegel, G.E. Scuseria, M.A. Robb, J.R. Cheeseman, J.A. Montgomery Jr., T. Vreven, K.N. Kudin, J.C. Burant, J.M. Millam, S.S. Iyengar, J. Tomasi, V. Barone, B. Mennucci, M. Cossi, G. Scalmani, N. Rega, G.A. Petersson, H. Nakatsuji, M. Hada, M. Ehara, K. Toyota, R. Fukuda, J. Hasegawa, M. Ishida, T. Nakajima, Y. Honda, O. Kitao, H. Nakai, M. Klene, X. Li, J.E. Knox, H.P. Hratchian, J.B. Cross, C. Adamo, J. Jaramillo, R. Gomperts, R.E. Stratmann, O. Yazyev, A.J. Austin, R. Cammi, C. Pomelli, J.W. Ochterski, P.Y. Ayala, K. Morokuma, G.A. Voth, P. Salvador, J.J. Dannenberg, V.G. Zakrzewski, S. Dapprich, A.D. Daniels, M.C. Strain, O. Farkas, D.K. Malick, A.D. Rabuck, K. Raghavachari, J.B. Foresman, J.V. Ortiz, Q. Cui, A.G. Baboul, S. Clifford, J. Cioslowski, B.B. Stefanov, G. Liu, A. Liashenko, P. Piskorz, I. Komaromi, R.L. Martin, D.J. Fox, T. Keith, M.A. Al-Laham, C.Y. Peng, A. Nanayakkara, M. Challacomb, P.M.W. Gill, B. Johnson, W. Chen, M. W. Wong, C. Gonzalez, J.A. Pople, Gaussian 03, Gaussian, Inc., Wallingford CT, 2004.
[19] Z-q. Liu, Q. Fang, D. Wang, G. Xue, W.-t. Yu, Z.-s. Shao, M.-h. Jiang, Chem. Commun. 23 (2002) 2900.